ISBN: 978-3-95450-234-9 ISSN: 2673-5504 doi:10.18429/JACoW-SRF2023-TUCBA01

MEASUREMENTS OF THE AMPLITUDE-DEPENDENT MICROWAVE SURFACE RESISTANCE OF A PROXIMITY-COUPLED Au/Nb BILAYER*

T. Oseroff†, M. Liepe, Z. Sun, CLASSE, Cornell University, Ithaca, NY, USA

Abstract

A sample host cavity is used to measure the surface resistance of a niobium substrate with a gold film deposited in place of its surface oxide. The film thickness of the gold layer was increased from 0.1 nm to 2.0 nm in five steps to study the impact of the normal layer thickness. The 0.1 nm film was found to reduce the surface resistance below its value with the surface oxide present and to enhance the quench field. The magnitude of the surface resistance increased substantially with gold film thickness. The surface resistance field-dependence appeared to be independent from the normal layer thickness. The observations reported in this work have profound implications for both low-field and high-field S.C. microwave devices. By controlling or eliminating the niobium oxide using a gold layer to passivate the niobium surface, it may be possible to improve the performance of SRF cavities used for particle acceleration. This method to reduce surface oxidation while maintaining low surface resistance could also be relevant for minimizing dissipation due to two-level systems observed in low-field low-temperature devices.

INTRODUCTION

The work presented at this conference is detailed in a paper for which we are currently seeking publication [1]. To avoid duplication, this paper will focus on a supplemental analysis regarding the expected thermal quench fields. As discussed in the main paper, the results of this analysis act as a crucial support for some of the work's main conclusions. As this is a supplementary writing, no attempt is made to introduce the details of the main work and the reader is assumed to be familiar with the information in [1].

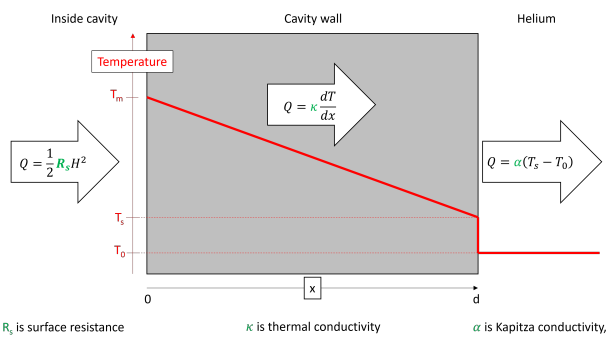

Figure 1: Diagram depicting system considered for model and defining relevant parameters and dimensions.

MODEL

A thermal quench occurs when the liquid helium surrounding the cavity is unable to adequately remove heating from the inner surface [2]. The physical situation consists of a 3 mm thick niobium bulk with a steady state heat flux, Q, created by an RF field, H, incident on one side and liquid helium cooling on the other. This scenario is demonstrated and relevant dimensions are defined in Fig. 1.

The analysis presented here closely follows that of Ref. [2] to obtain a steady-state estimate of the thermal quench field. Here it is assumed that the inner and outer surface temperatures are not increased substantially beyond that of the bath such that the thermal conductivity and Kapitza conductivity are approximately constant. This is likely not an ideal assumption for the frequencies considered in this work, but is sufficient for an initial consideration. From the steady-state heat flow at the metal-helium interface,

$$\kappa \frac{dT}{dx} = (T_s - T_0)\,\alpha.$$

All parameters included are defined in Fig. 1. Integrating both sides with respect to x from 0 to d yields an expression for T_s in terms of T_m

$$T_s = \frac{\alpha d T_0 + \kappa T_m}{\alpha d + \kappa}.$$

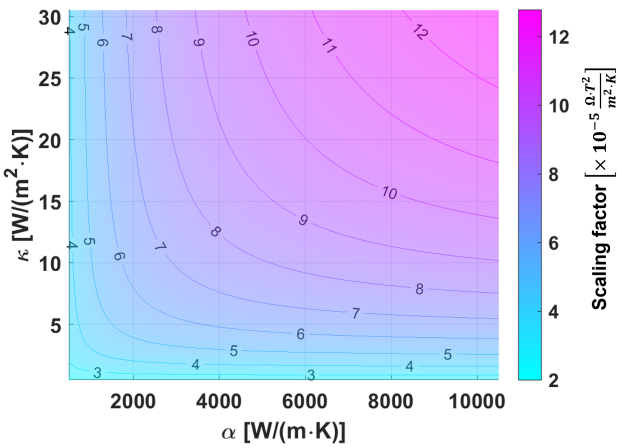

Figure 2: Scaling factor produced for a given combination of Kapitza conductivity and bulk thermal conductivity. Expected values include $\alpha = 1000 - 3000\,\mathrm{W/(m^2 \cdot K)}$ and $\kappa = 5 - 40\,\mathrm{W/(m \cdot K)}$ [3–5].

In the steady state, the heat flux into and out of the niobium will be equivalent:

$$\frac{1}{2\mu_0^2} R_s(T_m, B)|B|^2 = (T_s - T_0)\,\alpha.$$

* Work supported by Center of Bright Beams from the National Science Foundation under Grant No. PHY-1549132
† teo26@cornell.edu

ISBN: 978-3-95450-234-9 ISSN: 2673-5504 doi:10.18429/JACoW-SRF2023-TUCBA01

Combining this with the previous expression gives a relationship between T_m and the surface RF field, B:

$$R_s(T_m, B)|B|^2 = \left[2\mu_0^2 \frac{\alpha\kappa}{\alpha d + \kappa}\right](T_m - T_0) = S\,(T_m - T_0)\,. \quad (1)$$

Here the thermal properties are contained in the scaling factor, $S = 2\mu_0^2 \frac{\alpha\kappa}{\alpha d+\kappa}$. Figure 2 demonstrates what combination of the two material properties can produce a given scaling factor. The maximum field, B, for which a solution to Eq. (1) exists is the predicted thermal quench field [2].

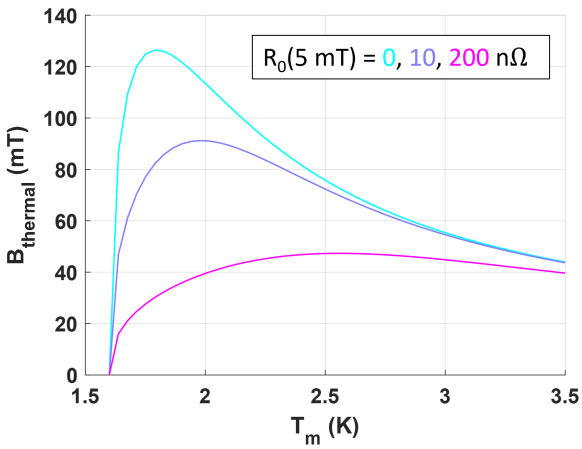

Figure 3: Solution to equation 1 with surface resistance modeled by Eq. (2) at a frequency of 4.0 GHz and a bath temperature of $T_0 = 1.6$ K. The scaling factor used in this figure is $S = 5\times10^{-5}\ \Omega\cdot\mathrm{T}^2/(\mathrm{m}^2\cdot\mathrm{K})$. The maximum values of each curve provide an estimate for the thermal quench field.

As was discussed in the primary paper [1], the gold layer samples all displayed a surface resistance varying with the square-root of RF field amplitude. The surface resistance used in Eq. (1) will be

$$R(T_m, B) = R_T\,(T_m) + R_0\,(B_0)\sqrt{\frac{B}{B_0}}, \quad (2)$$

where R_T denotes the temperature-dependent component of the surface resistance and B_0 is an arbitrary reference field. R_T will be obtained using the SRIMP model [6] with parameters obtained by fitting temperature-dependence data [7]. With such a surface resistance field-dependence, the solution to Eq. (1) is considered for several cases in Fig. 3. From this it is evident that for modest residual resistance contributions, the assumption that $T_m \approx T_0$ is reasonable for the purposes of assuming temperature-invariant thermal and Kapitza conductivities using the models cited in [3]. For larger residual resistance values this assumption should be refined for a more careful treatment.

APPLICATION TO DATA

The predicted thermal quenches can be compared to those observed in Ref. [1]. The data collected at 1.6 K is given in Fig. 4. Relevant information from this is summarized in Table 1.

Table 1: Measured quality factors at 5 mT and observed quench fields for the 4.0 GHz data in Fig. 4

Measurement	B_{quench} [mT]	$Q_0(5\,\mathrm{mT})[\times10^{10}]$
Oxidized Nb	73.8 ± 3.3	4.1
0.1 nm Au	105.0 ± 5.0	4.6
0.5 nm Au	67.6 ± 4.3	3.6
1.0 nm Au	57.8 ± 2.9	2.7
1.5 nm Au	43.8 ± 2.0	
2.0 nm Au	42.6 ± 4.3	1.7

In Fig. 5, Eqs. (1) and (2) are used to estimate the thermal quench field for a given total resistance at 1.6 K for a range of scaling factors. The possible range of resistances that can produce thermal quench fields within the uncertainty of the observed values is superimposed on top of the prediction for each measured surface.

For the majority of the measurements in Fig. 4, it is reasonable to assume that the quench location is on the sample plate due to the quench field changing magnitude when the sample surface is altered. This may or may not be true for the 0.1 nm Au sample. Regardless, it is assumed that the quench events occur on the sample surface and not on the host structure for all measurements considered here. In addition to this, it is assumed that there are no significant variations from the average surface resistance over its area. This is justified by the relatively large thermal quench fields obtained for reasonable material parameters [3, 5], which would likely not be obtained if dissipation were dominated by hot spots. To be more concise, it is assumed that the surface resistance on the plate and host structures are constant over their entire area.

With these assumptions in place, the average surface resistances on the plate and host structure that can produce the quality factors observed in Table 1 are plotted in Fig. 6. This is calculated from Eq. (1) in Ref. [1]. The surface resistances that could produce observed thermal quench fields in Fig. 5, assumed to be those of the plate, are superimposed on these calculations. This demonstrates what combination of average host and plate surface resistances could produce both the observed quality factor and thermal quench field for a given sample.

The value of scaling factor affects where the possible host resistances occur in Fig. 6. There, a value of $S = 5\times10^{-5}\ \Omega\cdot\mathrm{T}^2/(\mathrm{m}^2\cdot\mathrm{K})$ was selected as this allowed for all of the sample measurements to be consistent with a single host structure resistance. This is consistent with the expectation that the host structure resistance is invariant between different measurements. Other choices of scaling factor (outside about 10% of its value) rapidly become inconsistent with this expectation and often lead to impossible combinations of host and plate surface resistance. The selected value of $S = 5\times10^{-5}\ \Omega\cdot\mathrm{T}^2/(\mathrm{m}^2\cdot\mathrm{K})$ is consistent with thermal and Kapitza conductivities found in literature [3, 5], as can be observed in Fig. 2.

ISBN: 978-3-95450-234-9 ISSN: 2673-5504 doi:10.18429/JACoW-SRF2023-TUCBA01

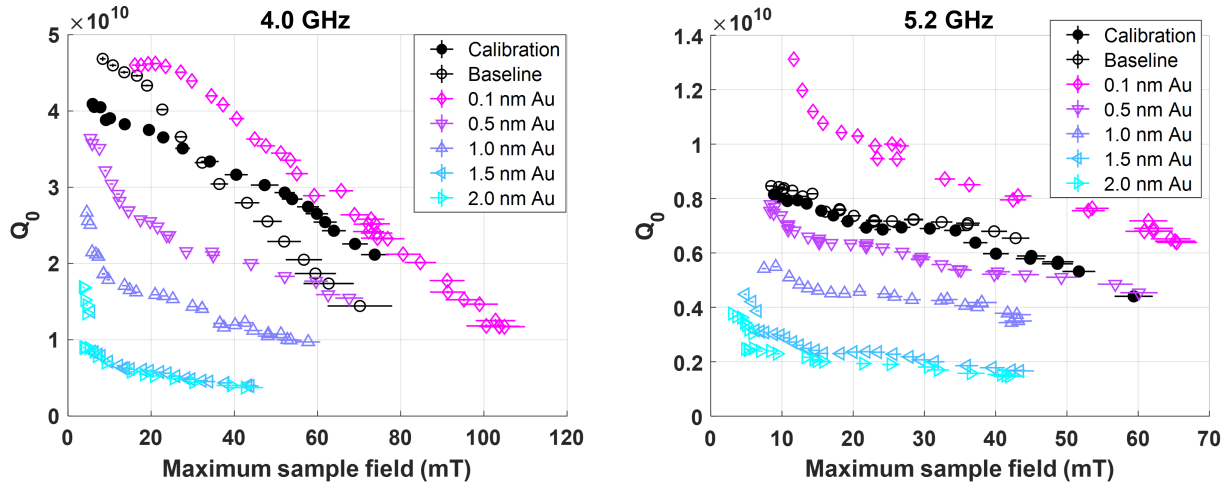

Figure 4: Intrinsic quality factors of niobium sample with its native oxide (baseline and calibration) and with gold layers of varying thickness. Measurements are given as a function of RF field magnitude on the sample at 1.6 K. This image is copied from Ref. [1] and further information is available there.

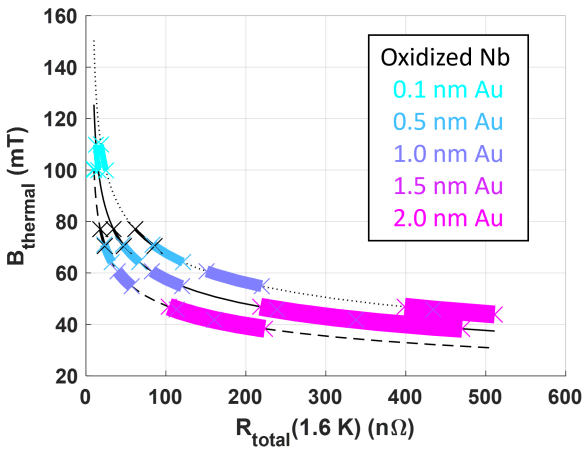

Figure 5: Predicted thermal quench fields from Eqs. (1) and (2) with scaling factors $S = 4, 5, 6 \left[\times 10^{-5}\ \Omega \cdot \mathrm{T}^2/(\mathrm{m}^2 \cdot \mathrm{K})\right]$ (dashed, solid, dotted black lines respectively). Each observed thermal quench field range, specified in Table 1, is superimposed on the associated predicted values.

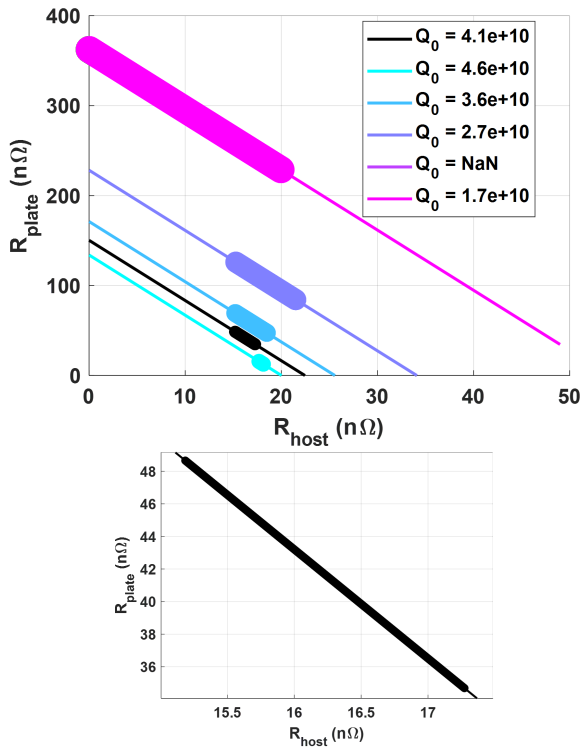

Figure 6: Average surface resistance on the host and plate that can result in a measured quality factor corresponding to the measurements in Table 1. This is calculated from Eq. (1) in Ref. [1]. Superimposed (thicker lines) over the range of plate surface resistances are the values of surface resistance that were consistent with thermal quench fields of each measurement considered in Fig. 5. A scaling factor of $S = 5 \times 10^{-5}\ \Omega \cdot \mathrm{T}^2/(\mathrm{m}^2 \cdot \mathrm{K})$ was selected such that the host structure surface resistance was consistent for all measurements. The lower figure is zoomed in on the oxidized niobium (calibration measurement) sample.

In the lower portion of Fig. 6, the allowed combination of plate and host resistance for the oxidized niobium sample is shown on a smaller scale to be viewed with more detail. From this, it appears that the host structure and plate must have different surface resistances to be consistent with the magnitude of the observed quench field. As described in in Ref. [1], this directly violates one of the core assumptions for surface resistance extraction using a calibrated quality factor measurement. From the temperature-dependencies presented in Ref. [1], the discrepancy is likely caused by an unknown form of residual resistance. Thus, this issue will become less pronounced for higher temperatures. At 1.6 K, however, it appears the surface resistance of the calibration plate could be two-three times that on the host structure.

ISBN: 978-3-95450-234-9 ISSN: 2673-5504 doi:10.18429/JACoW-SRF2023-TUCBA01

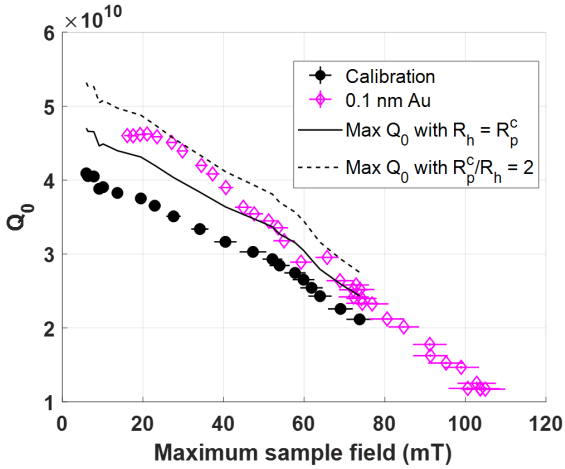

Figure 7: Maximum resonator Q_0 for a calibration plate with the assumed equivalence between the host and plate structures and allowing for some discrepancy. The calibration measurement and the 0.1 nm Au layer measurement are included for reference.

Allowing for this difference in the surface resistance extraction method specified in Ref. [1, 7] allows for a natural solution to some of the difficulties revealed by the 0.1 nm Au measurement. First, it explains how the quench field of the gold layer sample could be higher than that of the calibration. Second, the observed increase in quality factor following the removal of niobium oxide and its replacement with this gold layer was too large to be realized without the influence of systematic error. The surface resistance difference between the host and plate structures provides an explanation for this systematic error. The maximum possible quality factor corresponds to dissipation occurring solely on the host structure (i.e. the case where sample surface resistance is zero). This value can be obtained from modifications to equation 1 in Ref. [1] following from the derivation in Ref. [7] by allowing for a difference between plate and host structure resistances in the calibration measurement, denoted by $r = R_{plate}/R_{host}$:

$$Q_0^{max} = Q_0^{calibration}\left[1 + \frac{\alpha}{1-\alpha}r\right], \qquad (3)$$

where α is the focusing factor defined in Ref. [1]. The values reported here of $r = 2 - 3$ are consistent with the observed increase in magnitude. This is demonstrated in Fig. 7.

The same calculations and comparisons that were performed for 4.0 GHz in Fig. 5 can be repeated for the 5.2 GHz quench fields shown in Fig. 4 and listed in Table 2. This can then be expressed in terms of possible combinations of plate and host surface resistances, as was done for 4.0 GHz in Fig. 6. This is shown for the 5.2 GHz case in Fig. 8. The scaling factor of $S = 7 \times 10^{-5}\ \Omega \cdot \mathrm{T}^2/(\mathrm{m}^2 \cdot \mathrm{K})$ was selected such that the host structure surface resistance was most consistent for all measurements, though complete agreement was not obtained.

Table 2: Measured quality factors at 5 mT and observed quench fields for the 5.2 GHz data in Fig. 4

Measurement	B_{quench} [mT]	$Q_0(5\,\mathrm{mT})[\times 10^9]$
Oxidized Nb	59.4 ± 2.7	8.0
0.1 nm Au	65.4 ± 2.9	13
0.5 nm Au	60.1 ± 2.6	7.5
1.0 nm Au	43.2 ± 2.0	5.4
1.5 nm Au	43.4 ± 2.0	4.5
2.0 nm Au	41.2 ± 2.2	3.8

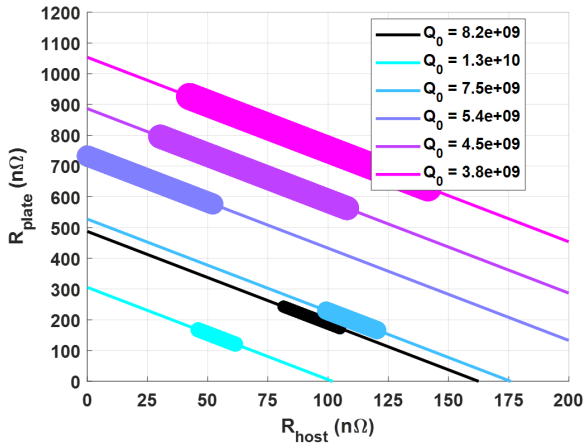

Figure 8: Repeating the process described for the 4.0 GHz case in Fig. 6 for the 5.2 GHz data. A scaling factor of $S = 7 \times 10^{-5}\ \Omega \cdot \mathrm{T}^2/(\mathrm{m}^2 \cdot \mathrm{K})$ was selected such that the host structure surface resistance were most consistent for all measurements.

This scaling factor is also inconsistent with the preferred value for the 4.0 GHz case. It is expected that this discrepancy is due to the initial assumption made in the model that the Kapitza conductivity and thermal conductivity were constant in temperature. For the 5.2 GHz case, and in general for the thicker gold layers, more dissipation was observed and temperatures inside the cavity wall may be large enough to justify dynamic behavior of these conductivities. This can be seen in Fig. 3. Additionally, the observed quadratic field-dependence of the oxidized niobium surface resistance was assumed to behave as a square-root here. Account for this would shift the behavior reported here slightly.

CONCLUSION

The information in this writing provides details supplementing the information presented at the conference and written in Ref. [1]. It is not intended to be a complete work and should be read after understanding [1]. It describes thermal models used to justify conclusions about the source of a systematic uncertainty that was revealed by the 0.1 nm gold layer measurement. These models produce thermal quench fields that are consistent with those observed with input parameters expected for niobium. However, the assumptions

ISBN: 978-3-95450-234-9 ISSN: 2673-5504 doi:10.18429/JACoW-SRF2023-TUCBA01

of the model may be too stringent, as fully consistent values were not obtained for both operation frequencies for a single set of material properties. This was likely due to the higher dissipation observed for higher frequencies and for the thicker gold layers. It is expected that this could be improved by implementing a more complete model that does not make these assumptions.

Despite the lack of complete consistency, the model is adequate to demonstrate that the mechanism of quench in these studies is a thermal breakdown field. It also provides a reasonable source of systematic error that was not ruled out by other observations and is capable of explaining the problematic differences between the gold layer measurement and the calibration measurement.

REFERENCES

[1] T. Oseroff, Z. Sun, and M. Liepe, "Measurements of the amplitude-dependent microwave surface resistance of a proximity-coupled au/nb bilayer," 2023. doi:10.48550/arXiv.2305.12035

[2] A. Gurevich, "Multiscale mechanisms of srf breakdown," *Physica C*, vol. 441, no. 1, pp. 38–43, 2006. doi:10.1016/j.physc.2006.03.024

[3] J. Ding, D. L. Hall, and M. Liepe, "Simulations of RF Field-induced Thermal Feedback in Niobium and Nb3Sn Cavities," in *Proc. SRF'17*, Lanzhou, China, Jul. 2017, pp. 920–924. doi:10.18429/JACoW-SRF2017-THPB079

[4] D. Hall, "New insights into the limitations on the efficiency and achievable gradients in Nb_3Sn SRF cavities," Ph.D. dissertation, Cornell University, 2017.

[5] R. Porter, "Advancing the maximum accelerating gradient of niobium-3 tin superconducting radio frequency accelerator cavities: Measurements, dynamic temperature mapping, and material growth," Ph.D. dissertation, Cornell University, 2021.

[6] J. Halbritter, *Fortran-program for the computation of the surface impedance of superconductors*, 1970. https://publikationen.bibliothek.kit.edu/270004230

[7] T. Oseroff, "Advancing a superconducting sample host cavity and its application for studying proximity-coupled normal layers in strong microwave fields," Ph.D. dissertation, Cornell University, 2022.